

# The oscillation modes of $\theta^2$ Tauri

## Results from the 1992 MUSICOS campaign\*

E.J. Kennelly<sup>1,2</sup>, G.A.H. Walker<sup>1</sup>, C. Catala<sup>3</sup>, B.H. Foing<sup>4</sup>, L. Huang<sup>5</sup>, S. Jiang<sup>5</sup>, J. Hao<sup>5</sup>, D. Zhai<sup>5</sup>, F. Zhao<sup>5</sup>, J.E. Neff<sup>6</sup>, E.R. Houdebine<sup>4</sup>, K.K. Ghosh<sup>7</sup>, and P. Charbonneau<sup>2</sup>

<sup>1</sup> Department of Geophysics and Astronomy, University of British Columbia, 129-2219 Main Mall, Vancouver, B.C., V6T 1Z4, Canada

<sup>2</sup> High Altitude Observatory, National Center for Atmospheric Research\*\*, P.O. Box 3000, 3450 Mitchel Lane, Boulder, CO, 80301, USA

<sup>3</sup> Observatoire Midi-Pyrénées, France

<sup>4</sup> ESA Space Science Department, ESTEC, The Netherlands

<sup>5</sup> Beijing Astronomical Observatory, Chinese Academy of Sciences, China

<sup>6</sup> Department of Astronomy and Astrophysics, Penn State University, USA

<sup>7</sup> Indian Institute of Astrophysics, Vainu Bappu Observatory, India

Received 9 November 1995 / Accepted 27 February 1996

**Abstract.** We have analyzed a series of 619 spectra of  $\theta^2$  Tauri taken with four telescopes over four consecutive nights during the 1992 global MUSICOS campaign. Radial velocity variations provide information about the oscillation frequencies of low degree ( $0 \leq \ell \leq 3$ ), and line-profile variations provide information on modes of higher degree ( $3 \leq \ell \leq 10$ ). The radial velocities were derived with a cross-correlation technique. In addition to detecting several frequencies found photometrically (e.g., Breger et al. 1989), we have found two new frequencies, which implies that the oscillation spectrum of  $\theta^2$  Tau may not be stable. Variations within rotationally broadened absorption lines were transformed by a Fourier-Doppler imaging analysis into a map of apparent frequency versus apparent azimuthal order. From this two-dimensional Fourier representation we identify some seven oscillation modes using a genetic algorithm to explore parameter space. While we find good agreement between the detected frequencies and those predicted to be unstable based on the models of Dziembowski (1990), it is still not clear why only certain modes are selected.

**Key words:** techniques: spectroscopic – binaries: spectroscopic – stars: individual:  $\theta^2$  Tauri – stars: oscillations –  $\delta$  Sct

Send offprint requests to: E.J. Kennelly

\* Based on observations obtained during the MUSICOS 92 Multi-Site Continuous Spectroscopic campaign from Beijing Observatory Xinglong 2.16m, Observatoire de Haute Provence 1.52m, William Herschel 4.2m, and National Solar Observatory McMath 1.5m telescopes.

\*\* The National Center for Atmospheric Research is sponsored by the National Science Foundation

### 1. Introduction

The  $\delta$  Scuti stars are  $1.5$  to  $2.5 M_{\odot}$  stars which lie within an extension of the Cepheid instability strip near the main sequence. The stars are found in both main sequence and more advanced stages of evolution and many are known to undergo multiperiodic oscillations. Consequently, the  $\delta$  Scuti stars are considered to be promising candidates for asteroseismological studies (Brown & Gilliland 1994). In theory, the oscillations would act as probes of the interior and could therefore be used to test theories of stellar structure and evolution.

Motivated by the prospect of seismology, the identification of frequencies and modes in  $\delta$  Scuti stars has become an extensive area of research in recent years. Especially successful have been the photometric campaigns lasting several weeks which have provided the necessary frequency resolution to reveal multiple modes of oscillation (e.g., Michel et al. 1992, Breger et al. 1995). Such studies are sensitive to the low-degree modes ( $0 \leq \ell \leq 3$ ) which may produce significant variations in integrated starlight. As many as 10 frequencies have been identified in several  $\delta$  Scuti stars using multi-site observations (Belmonte et al. 1993). However, as encouraging as this may seem, the theoretical frequency spectra of  $\delta$  Scuti stars can be, by comparison, extremely rich, especially for evolved objects (Dziembowski 1990). Thus, the identification of the relatively few observed modes based solely on the frequencies derived from photometric data is often difficult.

Fortunately, additional information about the oscillation frequencies and modes can be determined more or less directly from spectroscopic observations. If the star is rotating, the velocity variations on the stellar surface resulting from the non-radial oscillations are mapped onto Doppler-broadened absorption profiles (Vogt & Penrod 1983). Therefore, by analyzing

**Table 1.** Introducing  $\theta^2$  Tauri

---

- **Orbital Parameters** (This paper, Ebbighausen 1959, Peterson et al. 1993)
   
 $P = 140.738 \pm 0.008$  days     $\gamma = 37.93 \pm 0.08$  km s<sup>-1</sup>     $a \sin i = 0.377 \pm 0.002$  au
   
 $K = 29.4 \pm 0.1$  km s<sup>-1</sup>     $e = 0.750 \pm 0.002$      $f = 0.361 \pm 0.006 M_{\odot}$
- **Spectral Type** (Peterson et al. 1981, Peterson 1991, Peterson et al. 1993)
   
Primary:    A7IV     $v \sin i = 70 \pm 5$  km s<sup>-1</sup>
  
Secondary:    A5V     $v \sin i = 160 \pm 10$  km s<sup>-1</sup>
- **Temperature** of the system from photometry (Breger et al. 1989)
   
 $T_{eff,1} = 8200 \pm 100$  K     $\Delta T_{eff} = 100$  K
- **Magnitude** of the components from lunar occultations (Peterson et al. 1981)
   
 $V_{tot} = 3.41$      $\Delta V = 1.10 \pm 0.05$      $I_1/I_2 = 2.75$
- **Distance Modulus** to the Hyades (Gunn et al. 1988)
   
 $m - M = 3.28 \pm 0.26$
- **Composition** of the Hyades (VandenBerg & Poll 1989)
   
 $0.70 \leq X \leq 0.75$      $0.02 \leq Z \leq 0.03$
- **Evolutionary Stage and Mass** (Królikowska 1992)
   
Primary:    H-Shell Burning     $M = 2.63 \pm 0.01 M_{\odot}$ 
  
Secondary:    Main Sequence     $M = 2.23 \pm 0.01 M_{\odot}$
- **Photometric Variations** (Breger et al. 1987, Breger et al. 1989)
   
Freq. (c/d):    13.229653    13.480733    13.693597    14.317637    14.614537
   
Amp. (mag):    0.0066    0.0026    0.0045    0.0027    0.0012

---

the time variations of the “Doppler image”, information about the oscillation modes, including even those of high degree (i.e.,  $\ell \geq 3$ ), can be uncovered (e.g., Walker et al. 1987, Kennelly et al. 1992a). At the same time, the low-degree oscillations can be studied from radial velocity variations or as variations in the moments of the line profiles (e.g., Mantegazza et al. 1994).

One star that is particularly well-suited for study is the bright multiperiodic  $\delta$  Scuti star  $\theta^2$  Tauri. This object is both a spectroscopic binary and a member of the Hyades cluster and as a result, invaluable information about the star’s temperature, luminosity, composition, mass, and evolutionary status can be inferred observationally. Table 1 summarizes the known properties of the system. Although both components lie within the instability strip, the oscillations of  $\theta^2$  Tau are believed to originate with the primary of the system (Breger et al. 1989, Kennelly & Walker 1996). Intensive photometric observations (Breger et

**Table 2.** MUSICOS 92: observations of  $\theta^2$  Tau

---

Site	Reciprocal Dispersion (Å/pixel)	Resolution	Spectral Coverage (Å)	Exposure Times (sec)	S/N	No. of spectra
Xinglong	0.065	33000	33	600 – 900	100-200	74
OHP	0.033	47000	68	600 – 1200	100-300	65
WHT	0.042	46000	83	100 – 600	100-400	146
Kitt Peak	0.132	23000	106	100 – 300	300-500	334

---

al. 1987, Breger et al. 1989, and Kovács & Páparó 1989) have shown that  $\theta^2$  Tau oscillates with as many as five low-degree

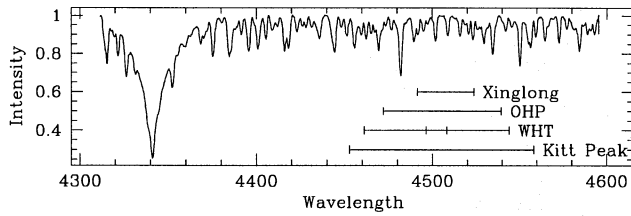


**Fig. 1.** The spectral region observed at each of the MUSICOS sites is indicated relative to a spectrum obtained at the Dominion Astrophysical Observatory. Two orders of the echelle data from WHT are indicated as overlapping regions.

modes separated by less than  $1.5 \text{ cycles day}^{-1}$ . Consistent frequencies and amplitudes were derived from each of these investigations, suggesting that the mode spectrum of  $\theta^2$  Tau is stable over a time scale of years. Observations obtained during one night at CFHT (Kennelly & Walker 1991, Kennelly & Walker 1996) demonstrated that line-profile variations owing to low- and high-degree oscillations are present in the spectra of  $\theta^2$  Tau. However, the CFHT observations lasted only five hours and were therefore insufficient to resolve the individual frequencies of this interesting star. Adequate resolution could only be achieved if observations were taken over several days. Moreover, because the frequencies of  $\theta^2$  Tau are very closely spaced, observations that are free of gaps are necessary to eliminate one-day aliases that could otherwise complicate the period analysis. Such observations are only possible through multi-site campaigns.

In this paper, observations of  $\theta^2$  Tau obtained during the second MUSICOS (MUlti-SItE COntinuous Spectroscopy) campaign are presented and analyzed.

## 2. The MUSICOS observations and reductions

MUSICOS is an international collaboration interested in areas of astronomical research requiring continuous, high-resolution spectroscopy (Catala et al. 1993). In 1992 December,  $\theta^2$  Tau was included as part of the second MUSICOS campaign. The purpose of the investigation was to monitor the line-profile variations within selected absorption lines (i.e., Ti II and Fe II at  $\lambda 4501$ ,  $\lambda 4508$  and  $\lambda 4515 \text{ \AA}$ ) and to use the observations to identify oscillation modes and frequencies. To this end, high-resolution spectra ( $R = 23000 - 47000$ ) of  $\theta^2$  Tau were collected using the 2.16 m telescope at the Xinglong Observatory in China, the 1.52 m telescope at the Observatoire de Haute Provence (OHP) in France, the 4.2 m William Herschel telescope (WHT) in the Canary Islands, and the 1.5 m McMath-Pierce telescope at Kitt Peak. The observations lasted for 4 days and are summarized in Table 2. Fig. 1 shows the spectral coverage for each of the sites relative to a spectrum of  $\theta^2$  Tau obtained at the Dominion Astrophysical Observatory prior to the campaign. Additional observations obtained at the Vainu Bappu Observatory in India were also successful but were made at a much lower resolution.

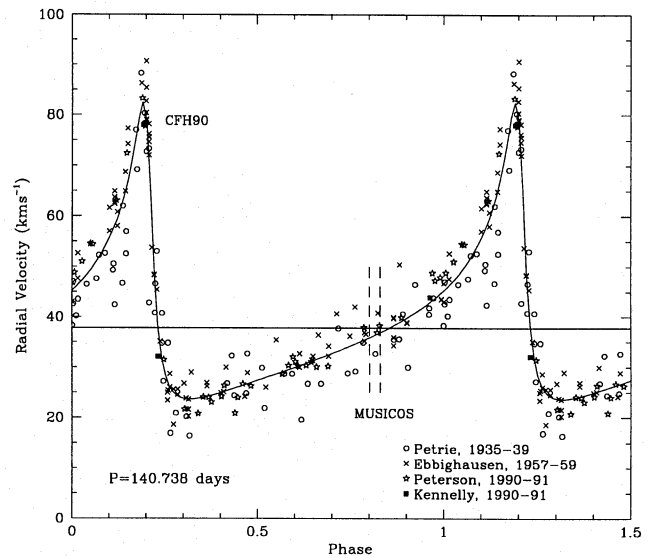


**Fig. 2.** The line-of-sight velocity of the primary star of the  $\theta^2$  Tau binary system was measured from observations obtained at CFHT and DAO and combined with those published in the literature to determine the orbital elements for the system. The data were phased to HJD 2424216.632 with the derived period of  $P = 140.738$  days. The phase during which the 1992 MUSICOS observations were obtained is indicated by the pair of dashed lines. Also indicated are the observations made at CFHT (CFH90; Kennelly & Walker 1996) when the stars were at their greatest velocity separation.

The MUSICOS observations of  $\theta^2$  Tau were coincident with a near-zero velocity shift between the binary components. In Fig. 2, the orbital radial velocity curve for the  $\theta^2$  Tau system is illustrated. Here, measurements derived from spectra obtained at CFHT (Kennelly & Walker 1995) and at the Dominion Astrophysical Observatory have been included with the published data from the radial velocity studies of Petrie (1940), Ebbighausen (1959), and Peterson et al. (1993). The orbital parameters listed in Table 1 were calculated from the combined data using the programs of Walker (1993), but the results differ little from those published by Peterson et al. The data have been phased using a period of  $P = 140.738$  days, and the curve of best fit is shown. Note that the orbit is highly eccentric. A pair of dashed lines separated by four days indicate the phase during which the 1992 MUSICOS observations were obtained. During the course of these observations, the radial velocity of the primary star changed by about  $1 \text{ km s}^{-1}$  due to the motion of the system. However, because the profiles of the secondary are quite broad ( $v \sin i \simeq 150 \text{ km s}^{-1}$ ) compared to that of the primary ( $v \sin i \simeq 75 \text{ km s}^{-1}$ ), the effect of this motion on the profiles of the primary should be negligible. (Note that this may not have been the case if the observations had been obtained during the phase when the relative velocity of the components is changing most rapidly.)

The phase coverage for the combined observations was extremely good, with a duty cycle of almost 80 percent. Therefore, one-day aliases which would normally be strong in observations

from a single site have been significantly reduced in the MUSICOS window function. Fig. 3 shows the window functions resulting from the individual and combined sites of the campaign.

The MUSICOS observations were reduced with IRAF<sup>1</sup> using standard techniques for two-dimensional CCD data. The bias (or dark) level was subtracted from each spectrum, and corrections for pixel-to-pixel variations were made by dividing the stellar spectra by a flat-field lamp. Afterwards, the data were extracted to produce a series of one-dimensional spectra. Cosmic-ray events were removed by manually editing each spectrum. The spectra were calibrated by taking a time-weighted average of the dispersion relations calculated from the Th-Ar spectra that preceded and succeeded the stellar observations, then corrected to a heliocentric reference frame. A correction for the orbital velocity of the primary was also applied to the observations. Finally, the spectra were normalized to unit continuum by first fitting the continuum of the mean spectrum from each site. Then the individual spectra were normalized by dividing each spectrum by the mean, fitting a low-order polynomial through the residuals, and dividing the spectra by the fitted functions. An additional site-dependent correction was determined and applied to the normalized spectra using the observations from the Vainu Bappu Observatory as a reference to ensure that the continuum for all the spectra was roughly the same.

### 3. Analysis of the radial velocity variations

Radial velocity variations provide information about the frequencies of low-degree modes ( $0 \leq \ell \leq 3$ ). Measurements of the radial velocity variations of  $\theta^2$  Tau were obtained using the IRAF cross-correlation routine; the results are illustrated in Fig. 4. Each panel in this figure shows the observations obtained during one day of the campaign. Observations from the four main sites are represented by different symbols. The amplitude of the variations is  $\sim 1 \text{ km s}^{-1}$  but seems to be modulated as though by beating. In a few instances, observations obtained at multiple sites were coincident. At these times, generally good agreement is found between the different measurements.

The Fourier amplitude spectrum was computed from the radial-velocity data using a routine for unequally spaced data (Matthews & Wehlau 1985) and is illustrated in Fig. 5. Confidence levels for the amplitude spectrum were calculated using the method of Bootstrap Resampling (Press et al. 1992). That is, the significance of a given peak was determined by comparing the Fourier amplitude spectrum of the actual observations to that of random data. In Fig. 5, the dashed line indicates the amplitude above which there is a 99% chance that the observed peaks do not result from random (white) noise. Several significant peaks can be identified and compared to the window function shown at the top of the figure. Due to the extremely

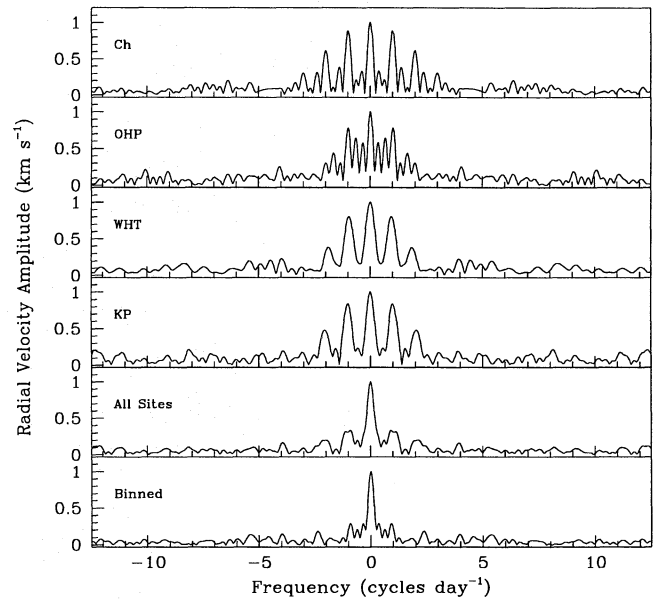


**Fig. 3.** The window functions for the individual (*Ch*, *OHP*, *WHT*, *KP*) and for the combined sites (*All Sites*) of the MUSICOS campaign are illustrated. Strong one-day aliases can be expected from the individual data sets but these are significantly reduced in the window function of the combined data set. The bottom figure (*Binned*) shows the window function for data after correcting for differences in time resolution (Sect. 3).

good time coverage, aliases should not complicate the analysis of this data too greatly.

The radial velocity data were analyzed using the following “cleaning” algorithm. The most significant peak was identified in the Fourier transform and the program PERDET (Breger 1980) was used to fit a sinusoidal function to the radial velocity measurements allowing the frequency, amplitude, and phase to vary. Once the best fit had been obtained, the data were pre-whitened by subtracting the derived periodicity from the data. The Fourier transform of the residuals was then examined to identify the frequency of the next most significant peak (relative to a recalculated 99% confidence level) and a new fit was made to the original data using two sinusoids. The procedure continued until no peak remained above the 99% confidence level within the frequency range from 0 to 25 cycles day<sup>-1</sup>. Four frequencies were derived with certainty from the data, although a solution invoking five frequencies was prompted by the appearance of a small residual variation at a frequency previously identified in the photometric studies. The results of the analysis are summarized in Table 3. In Fig. 4, the curve of best fit has been superimposed on the observations.

To test the validity of the derived solution, subsets of the radial velocity data were re-analyzed using the above procedure. First the observations were binned in time to produce effective integration times for all observations that were restricted between 10 and 20 minutes. In doing so, the effect of phase smearing on the radial-velocity amplitudes was made consistent at all sites and the number of spectra obtained from each

<sup>1</sup> IRAF is distributed by the National Optical Astronomy Observatories, which is operated by the Association of Universities for Research in Astronomy (AURA), Inc., under cooperative agreement with the National Science Foundation.

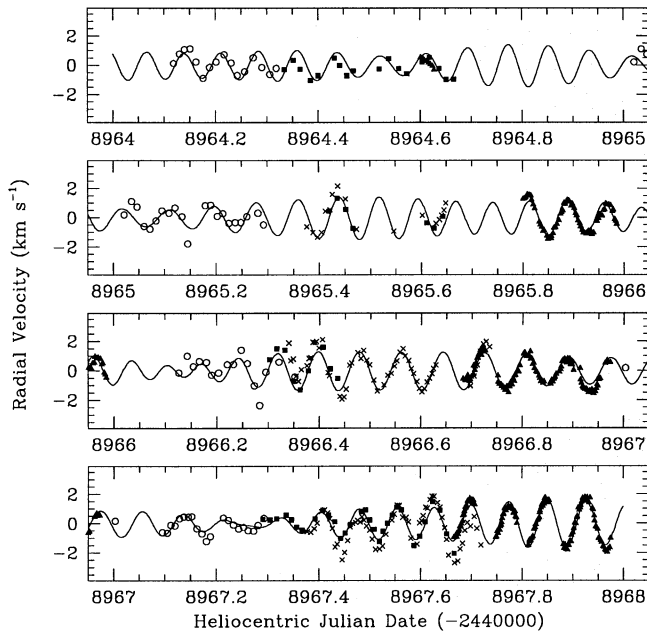


**Fig. 4.** Radial velocity shifts of the spectra relative to a mean spectrum for each site were measured using a cross-correlation routine. In this figure, the symbols have the following meaning: circle = Xinglong, square = OHP, cross = WHT, triangle = Kitt Peak. Good agreement is found between data sets during times when overlapping observations were obtained. The solid curve is the result of a sinusoidal fit to the data with five frequencies.

**Table 3.** Analysis of the radial velocity variations

Frequency (c/d):	11.75	12.32	13.25	13.71	14.33
Amplitude (km/s):	0.50	0.62	0.48	0.50	0.21

site became approximately equal. (In this way, would the observations from no one site dominate the solution of the Fourier spectrum.) The same five frequencies (in agreement to better than  $0.04 \text{ cycles day}^{-1}$ ) were derived from the subset. Analysis of the original velocity data while excluding in turn the data from each of the sites also confirmed the presence of the four dominant frequencies. However, when the data from each site were analyzed independently, only one frequency (usually the one at  $13.2 \text{ cycles day}^{-1}$ ) could be derived with any certainty. The difficulty encountered with the analysis of the single-site data, demonstrates the need for continuous observations.

In Fig. 6, the frequencies detected as velocity variations in the MUSICOS data are compared with the frequencies identified in the photometric observations of Breger et al. (1989). Variations at  $13.23$ ,  $13.69$ , and  $14.32 \text{ cycles day}^{-1}$  were identified in both sets of data but the MUSICOS observations failed to recover the frequencies at  $13.48$  and  $14.61 \text{ cycles day}^{-1}$ . These, however, had been detected with very low photometric ampli-

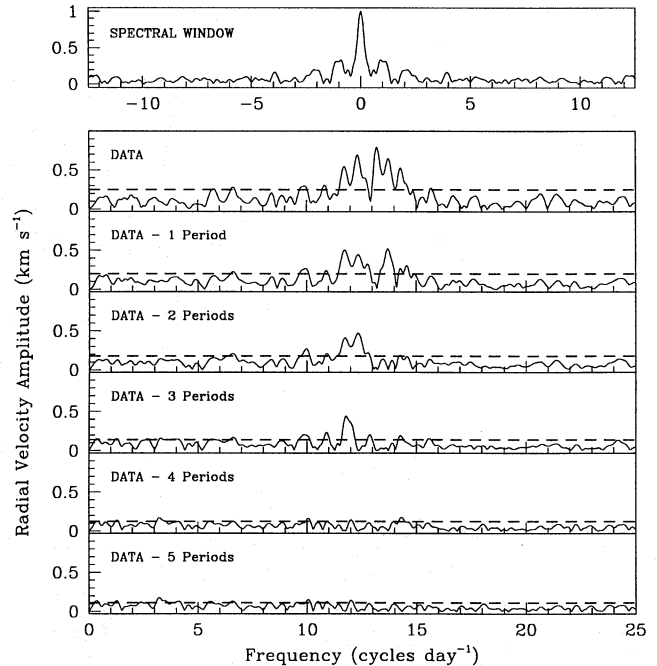


**Fig. 5.** The amplitude spectrum of  $\theta^2$  Tau is shown before and after the removal of each detected frequency. The spectral window function for the observations is shown at the top. The dashed line indicates the 99 % confidence level for the observations.

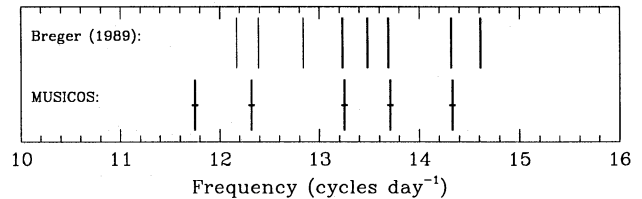


**Fig. 6.** The frequencies derived from the MUSICOS observations are compared with the results from the Breger et al. (1989) photometric campaign. Three of these frequencies agree very well with the photometric results. Two new frequencies identified in the MUSICOS data are supported by the identification of very low level variations found in a re-analysis of the photometric data (Hao 1994). The uncertainty in the MUSICOS frequencies is  $\pm 0.04 \text{ cycles day}^{-1}$ .

tudes. On the other hand, two new frequencies were discovered at  $11.75$  and  $12.32 \text{ cycles day}^{-1}$  from the MUSICOS observations. In a further analysis of the 1989 photometric data, Breger (1993) has noted evidence for power at lower (and higher) frequencies but with amplitudes below that which could be considered reliable. Also, in an independent analysis of the same photometric data, Hao (1994) identified peaks at  $12.17$ ,  $12.84$ , and  $12.39 \text{ cycles day}^{-1}$  with amplitudes not very different from the lowest-level variations cited by Breger et al. (1989). (That is, with photometric amplitudes of about one millimagnitude.) There is good reason therefore, to believe that all the frequencies detected in the MUSICOS data are intrinsic to the star. However for this to be the case, the amplitudes of the “new”

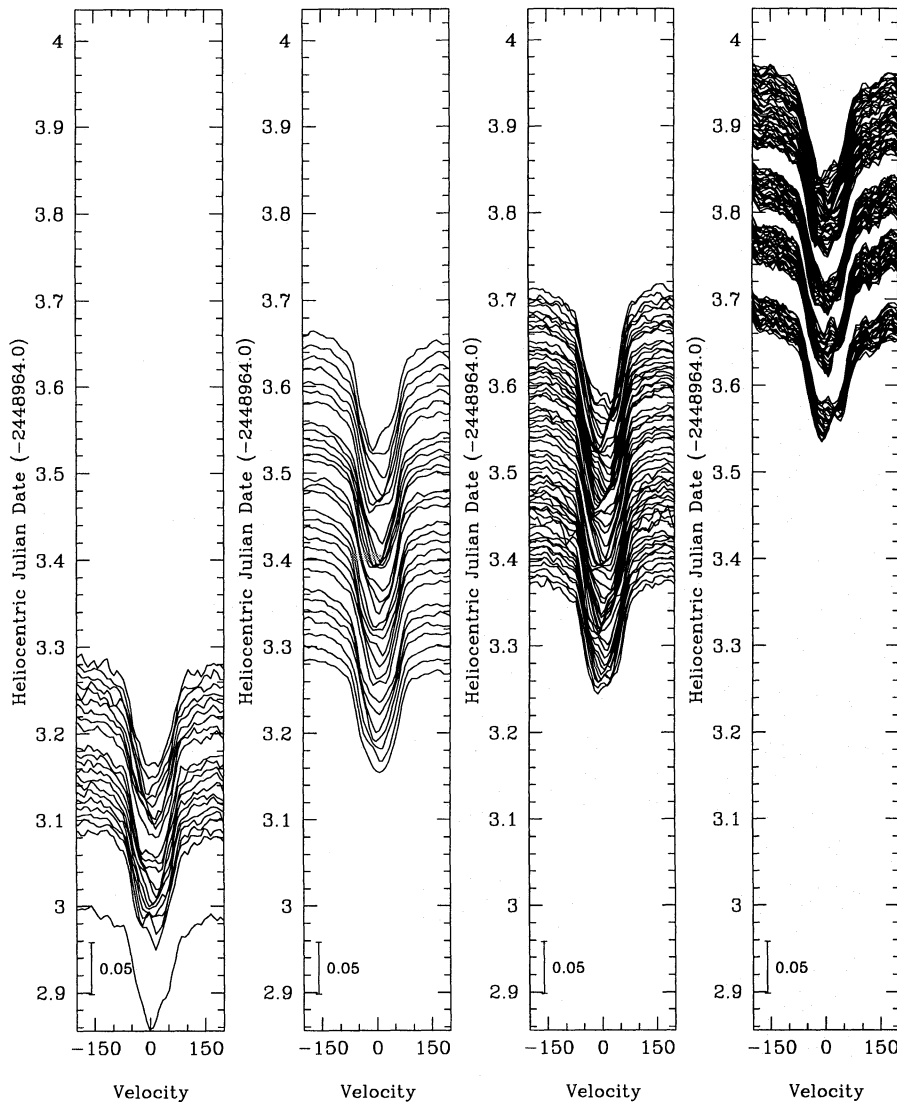


**Fig. 7.** The line-profile variations of  $\theta^2$  Tau are illustrated with spectra obtained (from left to right) at Xinglong, OHP, WHT, and Kitt Peak on the last day of the campaign (HJD 2448967 - 2448968). Time increases upwards and the intensity scale relative to a continuum of unity is specified by the error bar.

modes must have grown significantly during the 6 years since the photometric observations were obtained, since velocity-to-light ratios ( $2K/\Delta m$ ) of low-degree modes in  $\delta$  Scuti stars are typically expected between about 50 and 150 km s<sup>-1</sup> mag<sup>-1</sup> (Yang 1991).

#### 4. Analysis of the line-profile variations

Line-profile variations can provide direct information about both the frequencies and modes of oscillation. In Fig. 7, the time series of spectra obtained at each site on the last day of the campaign illustrate the line-profile variations of  $\theta^2$  Tau. Here, the information within three line profiles (at  $\lambda 4501$  Ti II,  $\lambda 4508$  Fe II, and  $\lambda 4515$  Fe II) has been averaged in order to improve the signal-to-noise ratio of the observations. The four panels show the data obtained at Xinglong, OHP, WHT, and Kitt Peak.

The variations were analyzed with the Fourier-Doppler Imaging (FDI) technique (Kennelly et al. 1992a). In that method, the time-variable component of the line profiles are transformed

in both time and Doppler space to produce a two-dimensional Fourier representation of the variations. In the resulting amplitude spectrum, the temporal frequencies are related to the frequencies of oscillation (and rotation), while the spatial frequencies can be identified with the azimuthal orders of the modes (assuming all modes are sectoral). For this reason, the two frequencies have been referred to as the apparent frequency ( $\hat{\nu}$ ) and the apparent azimuthal order ( $\hat{m}$ ). In reality, simulations have shown that the spatial frequency more closely represents the nonradial degree than it does the azimuthal order (Kennelly 1994), a fact first pointed out by Gough (1992). The simulations also indicated that the relationship between the mode of oscillation and its representation in Fourier space is not necessarily one-to-one, especially for the low-degree modes and this must be kept in mind when interpreting the Fourier spectra. A portion of the resulting Fourier amplitude spectrum of  $\theta^2$  Tau is illustrated as a grey-scale plot in Fig. 8. Here, the amplitudes are expressed as fractions of the continuum intensity. Although the frequency resolution is quite good ( $\Delta\hat{\nu} \simeq 0.25$  cycles day<sup>-1</sup>

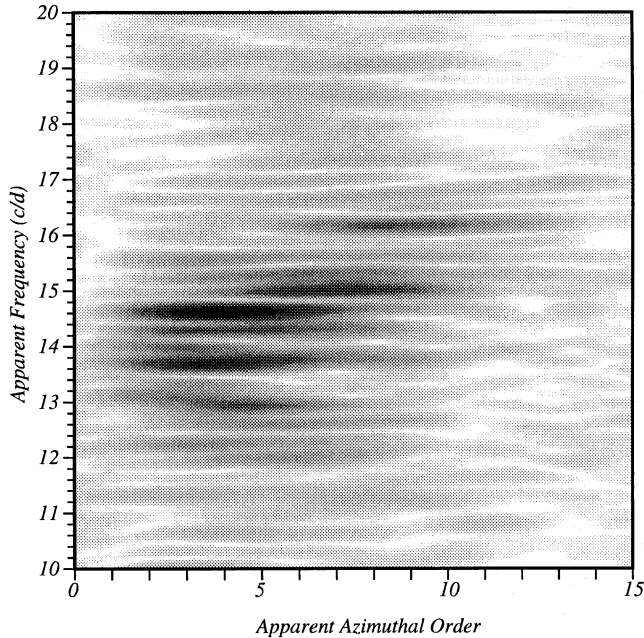


**Fig. 8.** The line-profile variations of  $\theta^2$  Tau were Fourier transformed in both space and time to produce this grey-scale map of the apparent azimuthal order versus apparent frequency of oscillation. The largest peak occurs at a frequency of 14.61 cycles day<sup>-1</sup> and has a maximum value of 0.0044 relative to a continuum of unity.

**Table 4.** Analysis of the line-profile variations

Frequency (c/d):	12.90	13.10	13.70	14.30	14.62	15.03	16.17
Azimuthal Order:	5.09	2.17	3.22	4.87	4.01	7.61	9.04
Amplitude	.0015	.0012	.0021	.0007	.0044	.0027	.0027

FWHM), the resolution in apparent azimuthal order is restricted by the fact that only half of the star can be observed and by the apodization of the variations which occurs in the wings of the profiles. For this reason, the peaks within the two-dimensional transform appear elongated in azimuthal order. (The FWHM of the peaks was measured to be approximately  $\Delta\hat{m} = 4$ .) In spite of this restriction, significant structure can be seen in the two-dimensional amplitude spectrum, not all of which can be attributed to the pattern of the window function.

Using the method of Bootstrap Resampling (as described in the previous section), the 99% confidence level for the oscillation spectrum was calculated to be 0.0010 relative to a continuum of unity within the range of frequencies and azimuthal orders illustrated in Fig. 8. Several peaks lying between 12 and 17 cycles day<sup>-1</sup> were identified with amplitudes above this level. The largest peak appears at  $\hat{m} \simeq 4.0$  and  $\hat{\nu} \simeq 14.6$  cycles day<sup>-1</sup> with an amplitude of 0.0044 relative to a continuum of unity. No significant peaks were found outside the illustrated range.

To identify all the independent modes of oscillations it was necessary to introduce an algorithm for fitting the oscil-

lation spectrum of  $\theta^2$  Tau in two dimensions. To expedite the calculation, the two-dimensional window function for the observations was approximated as the Fourier transform of the function  $W(\phi_j, t_i) = S(\phi_j)T(t_i)$ , where  $T(t_i) = 1.0$  and  $S(\phi_j) = 1.0 * \cos(\phi_j)$ . Here,  $(\phi_j, t_i)$  refer to the discretized coordinates of Doppler space and time for which observations exist. The cosine dependence on the spatial coordinate was introduced in order to emulate the amplitude dependence of the variations within the wings of the absorption lines. The two-dimensional amplitude spectrum of  $\theta^2$  Tau can then be modeled by scaling and shifting (in two directions) the window function to match each of the observed peaks. The method is somewhat analogous to the one-dimensional analysis of Fourier spectra by Gray & Desikachary (1973).

Alternatively, the minimization problem can be expressed in terms of the profile variations directly. In this case, the time-variable component of the line-profile variations is approximated as sum of a number of sinusoidal variations in time and space multiplied by the appropriate apodizations. Then, in addition to the amplitudes and frequencies (both temporal and spatial), the phases can also be determined. In the event that some frequencies may lie close to the aliases of another, the inclusion of this parameter may have some consequence on the solution.

The observations were automatically searched for up to 10 independent modes using an early version of the genetic algorithm-based optimization subroutine PIKAIA (Charbonneau 1995). The genetic algorithm invokes principles of biological evolution and natural selection to search parameter space for the best solution using a population of trial solutions. In this case, the parameters to be determined (i.e., the frequencies, apparent azimuthal orders, amplitudes, and phases of the 10 modes) are encoded as the ‘genes’ of each population member. The fitness of the population members is then described as a  $\chi$ -squared statistic, calculated either from the difference between the modeled and observed Fourier amplitude spectra or from the corresponding line profile variations. The best-fit model is obtained by allowing the population members to ‘breed’ over successive ‘generations’ with the probability of a population member being picked for breeding made proportional to the individual’s ‘fitness’ as measured by the  $\chi$ -squared statistic.

The genetic-optimization routine converges to a solution with reasonable swiftness in the case of either minimization problem and the resulting optimal model parameters are similar. However, neither representation is ideal because of the approximations introduced in the models (i.e., the lack of phase information in the case of the Fourier fit and the ad hoc description of the apodization function in the case of the fit to the residuals.) Better results were obtained by minimizing the difference between modeled and observed profile variations and Fourier amplitude spectra simultaneously. Table 4 summarizes the results. The uncertainties in the derived frequencies were estimated to be  $\pm 0.05$  cycles day<sup>-1</sup>. All but one of the modes listed in the table have amplitudes (expressed as a fraction of the continuum intensity) that are above the 99% confidence level for the observations. In Fig. 9, a “cleaned” version of the two-

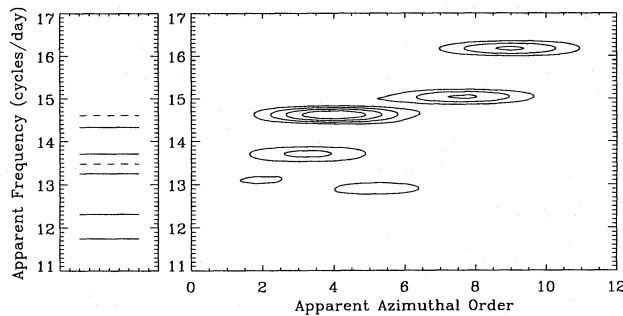


**Fig. 9.** A “cleaned” version of the transformed line-profile variations shows the location of the largest peaks identified in Table 4. For comparison, the frequencies derived from the radial velocity analysis of the MUSICOS data (together with those identified by Breger et al. (1989)) are illustrated to the left of the plot.

dimensional Fourier amplitude spectrum is presented as a contour plot, showing the peaks identified in Table 4.

Among the modes and frequencies derived by this analysis, of principle note are the two largest low-degree variations and two largest high-degree variations. The variation at  $14.62 \text{ cycles day}^{-1}$  appears with the largest amplitude at an apparent azimuthal order that could possibly correspond to a low-degree mode (i.e., be detected with photometry). The frequency of this variation agrees very well with the highest frequency identified during the photometric campaigns (at  $14.61 \text{ cycles day}^{-1}$ ). Similarly, the variation detected at  $13.70 \text{ cycles day}^{-1}$  seems to match the frequency of the low-degree mode identified in both the photometric observations (at  $13.69 \text{ cycles day}^{-1}$ ) and the radial-velocity analysis of the MUSICOS data (at  $13.71 \text{ cycles day}^{-1}$ ). The other low-degree modes, detected either as photometric or radial-velocity variations, do not seem to produce large-amplitude line-profile variations. However, two high-degree variations appearing with somewhat higher frequencies at  $15.03$  and  $16.17 \text{ cycles day}^{-1}$  are quite prominent. The appearance of the largest of these frequencies is consistent with the high-degree variation discovered by Kennelly & Walker (1996) at  $\hat{m} \simeq 9.3$  and  $\hat{\nu} \simeq 16.0 \text{ cycles day}^{-1}$ .

## 5. Discussion

$\theta^2$  Tauri is a spectroscopic binary with both the primary and secondary stars falling within the  $\delta$  Scuti instability strip. Calculations of the light-time delay due to the binary orbit (e.g., Breger et al. 1989) and an analysis of line profile variations while the two components were at their greatest velocity separation (Kennelly & Walker 1996) has indicated that the variability of  $\theta^2$  Tau originates with the primary of the system. Królikowska (1992) developed an evolutionary sequence of models to describe the observed properties of the binary components and concluded that the primary must exist in an evolved stage of main-sequence evolution or in the hydrogen-shell burning stage. Being an evolved star,  $\theta^2$  Tau is expected to have an extremely rich frequency spectrum because, in addition to acoustic modes (or p modes) trapped near the surface, numerous gravity modes

(or g modes) will be free to propagate deep within the star (Dziembowski 1990). Though the region of g-mode propagation is far from the surface, for low-degree p modes the evanescent region separating the g-mode propagation zone from that of the p modes is narrow. Thus g modes could interact with the p modes and might even reach observable amplitudes at the surface. Past investigations have sought an explanation of the frequency spectrum of  $\theta^2$  Tau in terms of nonradial p modes (e.g., Breger et al. 1989). Though p modes still seem the most likely explanation for the observed variations, the possibility that g modes might appear with detectable surface amplitudes can not be dismissed. For example, Breger et al. (1995) has suggested a solution to the frequency spectrum of FG Vir that includes g modes, though it was admitted that the solution was not unique with only 10 percent of the theoretically unstable modes with  $\ell \leq 2$  being observed.

The observed spectrum of  $\theta^2$  Tau is typical of  $\delta$  Scuti stars in that it exhibits only a handful of low-degree modes while many more are predicted to be unstable. The majority of the observed frequencies are very closely spaced (albeit there may be evidence for low-level variations at higher frequencies (Breger 1993)). From the information provided in Table 1, the following properties can be inferred for the primary of the  $\theta^2$  Tau system:  $L \simeq 56L_{\odot}$ ,  $T_{\text{eff}} \simeq 8200 \text{ K}$ ,  $M \simeq 2.6M_{\odot}$ , and  $R \simeq 3.7R_{\odot}$ . From these values and using the models of Dziembowski (1990), the range of frequencies spanned by unstable radial modes can be determined. Though the numbers are uncertain, unstable modes are expected between  $11.5$  and  $14.5 \text{ cycles day}^{-1}$  in the case of Helium-normal abundances and between  $9.0$  and  $17.0 \text{ cycles day}^{-1}$  in the case of Helium-rich abundances. Agreement with the observed range of frequencies is very good. However, since the period ratio between the first harmonic and the fundamental mode is  $P_1/P_2 = 0.77$ , while the period ratio for the next two harmonics is  $P_2/P_1 = 0.81$  (Breger 1989), it is unlikely that the observed mode spectrum of  $\theta^2$  Tau includes more than one (or two) radial modes.

Past observations of  $\theta^2$  Tau (i.e., Breger et al. 1987, Breger et al. 1989, and Kovács & Paparó 1989) have revealed frequencies and amplitudes that seem to be stable over time scales of months or years. However, the discovery of two new large amplitude variations derived from the MUSICOS data (taken six years after the last photometric results) now suggests that this is not the case. In fact, long-term amplitude variability is common property among  $\delta$  Scuti stars (Breger 1991). The explanation for the short mode lifetimes and relatively sparse spectra is thus far unknown. Currently, the most promising suggestion is that resonant mode coupling between p modes at the surface and g modes in the interior is somehow responsible for the selection of modes (Dziembowski 1990). However, because of the complexity of the problem, the theory is able to make few predictions regarding the expected mode spectrum.

The MUSICOS observations reveal that the number of high-degree modes excited in  $\theta^2$  Tau are also few, with only two periodicities at approximately  $\ell = 7$  and  $9$  being easily detected. This lack of high-degree variability may have implications for the problem of mode selection. The zone of propagation of the



high-degree modes  $i$ s well separated from the interior by a wide evanescent region. Therefore, interaction between modes in the core and high-degree modes at the surface are not expected. Still some kind of mode selection seems to take place. There is no evidence of rotational splitting among the high-degree modes of  $\theta^2$  Tau and, like other line-profile variables (e.g.,  $\tau$  Peg; Kennelly et al. 1992a,  $\kappa^2$  Boo; Kennelly et al. 1991,  $\gamma$  Boo Kennelly et al. 1992b, and  $\nu$  UMa; Korzennik et al. 1995), the frequency of the high-degree modes observed in  $\theta^2$  Tau tend to increase with nonradial degree (or apparent azimuthal order). Kennelly et al. (1992a) suggested that the spectrum of high-degree modes in the star  $\tau$  Peg could be interpreted as a series of prograde, sectoral modes each with approximately the same frequency in the corotating frame of the star. A similar interpretation could also be proposed to explain the variations of  $\theta^2$  Tau (Kennelly & Walker 1996) but why prograde sectoral modes should be preferred is unclear. Nevertheless, that rotation can influence the mode-spectra of  $\delta$  Scuti stars is well documented by the fact that slowly rotating  $\delta$  Scuti stars tend to oscillate with just one or two radial modes while rapidly rotating stars tend to support multiperiodic nonradial oscillations (Breger 1991).

To identify the low-degree modes of oscillation from the MUSICOS observations, we consider together the spectrum of modes detected as line-profile, radial velocity, and photometric variations. For example, the variation found at  $\sim 14.61$  cycles  $\text{day}^{-1}$  was observed with a very low amplitude photometric variation but as large amplitude line-profile variations. At the same time, the mode did not produce a signal that could be detected in the radial velocity analysis. In order for this to be the case, the degree of the mode must be fairly high (i.e.,  $\ell \geq 3$ ). However, to be detected photometrically the degree of the mode must be low (i.e.,  $\ell \leq 3$ ). Therefore, provided the detected signals have the same origin, the only explanation that seems possible is that the variation detected at  $14.61$  cycles  $\text{day}^{-1}$  results from a (sectoral)  $\ell = 3$  mode. If this assessment is correct, it implies that modes as high as  $\ell = 3$  can be (and are being) detected with ground-based photometric observations, so all modes with  $\ell = 0$  to 3 should be considered when attempting to interpret the photometric frequency spectra of  $\delta$  Scuti stars. Very often modes as high as  $\ell = 3$  are neglected in such analyses under the assumption that these modes are less likely to be detected because the cancellation effects of the variations observed in integrated starlight will be greater for these modes than for modes of lower degrees (e.g., Goupil et al. 1993).

Unfortunately, the identification of the remaining modes is less clear cut. The frequency at  $\sim 13.70$  cycles  $\text{day}^{-1}$  has been identified from variations in line-profiles, radial-velocity, and photometry and the most likely explanation of this mode may be as a (sectoral)  $\ell = 2$  mode. The remaining modes, detected as either radial velocity or light variations, produce no obvious signal of line-profile variations, so the identification of these modes is even less certain. Possibly some of these are rotationally split components of the same  $\ell = 3$  or  $\ell = 2$  modes identified above. To first order, the rotation of  $\theta^2$  Tau is expected to introduce frequency splittings with an amplitude of  $\Delta\nu \simeq 0.4$  cycles  $\text{day}^{-1}$ , assuming the star is seen nearly equator-on. The

separation between several of the observed modes is of this magnitude. However, the second-order effects of rotational splitting are non-negligible for  $\delta$  Scuti stars but they can be taken into account using the formula of Saio (1981) (assuming uniform rotation) and Dziembowski & Goode (1992) (allowing for differential rotation). The formalism of Dziembowski & Goode is especially important for evolved stars for which interactions between p and g modes may occur. Though some interesting coincidences can be found (e.g., the variations at  $14.32$  and  $13.48$  cycles  $\text{day}^{-1}$  are consistent with tesseral components of the proposed  $\ell = 3$  and  $\ell = 2$  modes), in general rotational splittings (as described by Saio) can not account for the observed mode spectrum of  $\theta^2$  Tau.

With the addition of the MUSICOS observations,  $\theta^2$  Tau is almost certainly the most intensely investigated  $\delta$  Scuti star to date. Even so the mode spectrum of this star remains for the most part unsolved. While additional observations (already carried out during 1994 in the form of a simultaneous photometric and spectroscopic campaign) may reveal more about this interesting star (especially if the amplitude spectrum is changing), efforts to explain the observed spectrum with detailed theoretical models are clearly required. In light of the unique information provided by the MUSICOS observations, these models should be able to account for all the observed modes ranging from  $\ell = 0$  to 10.

*Acknowledgements.* We wish to thank the staffs of the Xinglong 2.16 m telescope, the OHP 1.52 m telescope, the 4.2 m William Herschel telescope, the 1.5 m McMath-Pierce telescope, the 1 m Vainu Bappu telescope, and the Dominion Astrophysical Observatory 1.2 m telescope for their assistance during the observations. This research was supported in part by funding from the National Sciences and Engineering Research Council of Canada.

## References

- Belmonte, J.A., Roca Cortés, T., Vidal, I., et al. 1993, in *Inside the Stars*, IAU Colloquium 137, ASP Conference Series, Vol 40, eds. W.W. Weiss and A. Baglin, p. 739
- Breger, M. 1980, *ApJ*, 237, 850
- Breger, M. 1989, *Delta Scuti Star Newsletter*, 1, 7
- Breger, M. 1991, *A & A*, 270, 107
- Breger, M. 1993, in *New Perspectives on Stellar Pulsation and Pulsating Variable Stars*, IAU Colloquium 139, eds. J. Nemeč and J.M. Matthews (Cambridge University Press), p. 135
- Breger, M., Garrido, R., Huang, L., et al. 1989, *A & A*, 214, 209
- Breger, M., Handler, G., Nather, R.E., et al. 1995, *A & A*, 297, 473
- Breger, M., Huang, L., Jiang, S., et al. 1987, *A & A*, 175, 117
- Brown, T.M. and Gilliland, R.L. 1994, *ARA&A*, 32, 37
- Catala, C., Foing, B.H., Baudrand, J., et al. 1993, *A & A*, 275, 245
- Charbonneau, P. 1995, *ApJS*, 101, 309
- Dziembowski, W. 1990, in *Progress of Seismology of the Sun and Stars*, eds. Y. Osaki and H. Shibahashi, (Springer), p. 359
- Dziembowski, W.A. and Goode, P.R. 1992, *ApJ*, 394, 670
- Ebbighausen, E.G. 1959, *PASP*, 11, 235
- Gough, D. 1992, private communication
- Goupil, M.J., Michel, E., Lebreton, Y., and Baglin, A. 1993, *A & A*, 268, 546
- Gray, D.F. and Desikachary, K. 1973, *ApJ*, 181, 523

- Gunn, J.E., Griffin, R.F., Griffin, R.E.M., and Zimmerman, B.A. 1988, AJ, 96, 172
- Hao, J. 1994, private communication
- Kennelly, E.J. 1994, Ph.D. Thesis, University of British Columbia
- Kennelly, E.J. and Walker, G.A.H. 1991, Canada-France-Hawaii Information Bulletin, 25, p. 17
- Kennelly, E.J. and Walker, G.A.H. 1996, PASP, submitted
- Kennelly, E.J., Walker, G.A.H., and Hubeny, I. 1991, PASP, 103, 1250
- Kennelly, E.J., Walker, G.A.H., and Merryfield, W.J. 1992a, ApJ, 400, L71
- Kennelly, E.J., Yang, S., Walker, G.A.H., and Hubeny, I. 1992b, PASP, 104, 15
- Korzennik, S., Noyes, R., Brown, T., Nisenson, P., and Horner, S. 1995, ApJ, 443, L25
- Kovács, G. and Paparó, M. 1989, MNRAS, 237, 201
- Królikowska, M. 1992, A & A, 260, 183
- Mantegazza, L., Poretti, E., and Bossi, M. 1994, A & A, 287, 95
- Matthews, J.M. and Wehlau, W. H. 1985, PASP, 97, 841
- Michel, E., Belmonte, J.A., Alvarez, M., et al. 1992, A & A, 255, p. 139
- Peterson, D.M. 1991, in The Formation and Evolution of Star Clusters, ASP Conference Series, Vol 13, ed. K. Janes, p. 592
- Peterson, D.M., Baron, R.L., Dunham, E., and Mink, D. 1981, AJ, 86, 1090
- Peterson, D.M., Stefanik, R.P., and Latham, D.W. 1993, AJ, 105, 2260
- Petrie, R.M. 1940, PASP, 52, 286
- Press, W.H., Flannery, B.P., Teukolsky, S.A., and Vetterling, W.T. 1992, Numerical Recipes, second edition (Cambridge University Press), p. 684
- Saio, H. 1981, ApJ, 244, 299
- VandenBerg, D.A. and Poll, H.E. 1989, AJ, 98, 1451
- Vogt, S.S. and Penrod, G.D. 1983, ApJ, 275, 661
- Yang, S. 1991, in Rapid Variability of OB-Stars: Nature and Diagnostic Value, ed. D. Baade, ESO Conference and Workshop Proceedings, 36, p. 129
- Walker, A. 1993, M.Sc. Thesis, University of British Columbia
- Walker, G.A.H., Yang, S., and Fahlman, G.G. 1987, ApJ, 320, L139